

# Performance of COVQ over AWGN/Rayleigh Channels with Soft-Decision BPSK Modulation<sup>†</sup>

Nam Phamdo\* and Fady Alajaji<sup>‡</sup>

\*Department of Electrical Engineering  
State University of New York at Stony Brook, Stony Brook, NY 11794-2350

<sup>‡</sup>Department of Mathematics and Statistics  
Queen's University, Kingston, Ontario K7L 3N6, Canada

## ABSTRACT

A channel-optimized vector quantizer (COVQ) scheme that exploits the channel soft-decision information is proposed. The scheme is designed for stationary memoryless Gaussian and Gauss-Markov sources transmitted over BPSK-modulated additive white Gaussian noise (AWGN) or Rayleigh fading channels. It is demonstrated that coding gains of up to 2 dB can be achieved at low channel signal-to-noise ratios over COVQ systems designed for discrete (hard-decision demodulated) channels. Finally, this scheme is compared with the soft Hadamard column decoder of Skoglund and Hedelin.

## 1. INTRODUCTION

Recent works [1]–[9] on combined source-channel coding show that significant performance improvement can be realized for very noisy communication channels. Most of these works (with the exception of [9]) deal however with discrete channel models – i.e., channels used in conjunction with hard-decision demodulation.

In this paper, we incorporate the use of soft-decision information in the design of combined source-channel coding schemes. More specifically, we propose a channel-optimized vector quantizer (COVQ) [1, 2, 3] for additive white Gaussian noise (AWGN) and Rayleigh fading channels with soft-decision binary phase-shift keying (BPSK) modulation. This scheme – which consists of a source code designed for noisy channels – is in many ways similar to channel coding techniques that employ soft-decision coded modulation. Numerical results indicate that coding gains of up to 2 dB can be achieved over COVQ systems designed for hard-decision demodulated channels.

This work is also closely related to the soft Hadamard column decoder (SHCD) of [9]. However, the computation complexity of the decoder in this paper is much less than that of [9] – although the memory requirement is stronger.

<sup>†</sup>The work of Phamdo (phamdo@sbee.sunysb.edu) was supported in part by NTT Corporation. The work of Alajaji (fady@polya.mast.queensu.ca) was supported in part by an ARC grant, Queen's University.

## 2. DMC CHANNEL MODEL

The proposed system is illustrated in Figure 1. The input source,  $\mathbf{v}$ , is a  $k$ -dimensional real vector, and the COVQ operates at a rate of  $r$  bits per source dimension. For each input vector, the encoder produces a binary vector  $\mathbf{x} \in \{0, 1\}^{kr}$  for transmission. Each of the  $kr$  bits of  $\mathbf{x}$  is BPSK modulated, and the output,  $\mathbf{w} \in \{-1, +1\}^{kr}$ , is transmitted over an AWGN channel according to

$$z_i = w_i + n_i, \quad i = 1, 2, \dots, kr,$$

where  $w_i \in \{-1, +1\}$  is the BPSK signal of unit energy, and  $n_i$  is a zero-mean Gaussian random variable with variance  $N_0/2$  (we assume that  $n_i$  and  $n_j$  are independent for  $i \neq j$ ).

At the receiver, each received vector,  $\mathbf{z}$ , is demodulated with  $q$ -bit soft decision (through the use of a uniform scalar quantizer) yielding  $\mathbf{y} \in \{0, 1\}^{qkr}$ . Thus, for each  $k$ -dimensional source vector,  $qkr$  bits are produced at the demodulator output. These bits are then passed to the COVQ decoder.

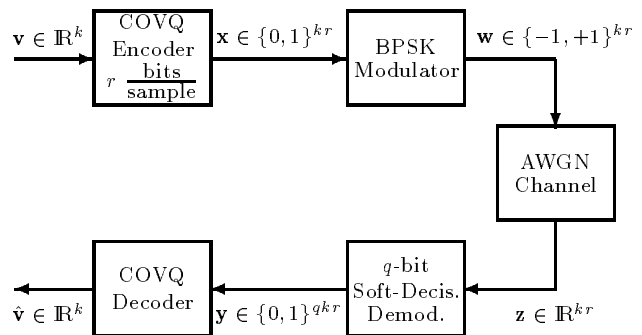


Figure 1. Block Diagram of the System.

We note that the concatenation of the modulator, channel, and demodulator constitutes indeed a  $2^{kr}$ -input,  $2^{qkr}$ -output discrete memoryless channel (DMC). This channel is equivalent to a binary-input,  $2^q$ -output DMC used  $kr$  times. Its channel transition probability matrix can hence be computed from the channel signal-to-noise ratio ( $SNR$ ) and the complementary error function. More specifically,

if

$$\mathcal{X} = \{0, 1\}$$

and

$$\mathcal{Y} = \{0, 1, 2, \dots, 2^q - 1\},$$

then the transition probability matrix  $\mathbf{\Pi}$  is given by

$$\mathbf{\Pi} = [\pi_{ij}], \quad i \in \mathcal{X}, j \in \mathcal{Y},$$

where

$$\begin{aligned} \pi_{ij} &\triangleq P(Y = j | X = i) \\ &= Q\left(\frac{(T_{j-1} - (2i - 1))\sqrt{SNR}}{1}\right) \\ &\quad - Q\left(\frac{(T_j - (2i - 1))\sqrt{SNR}}{1}\right), \end{aligned}$$

where  $SNR = \frac{E[w^2]}{E[n^2]} = \frac{2}{N_0}$  is the channel signal-to-noise ratio,

$$Q(x) = \frac{1}{\sqrt{2\pi}} \int_x^\infty \exp\{-t^2/2\} dt$$

is the complementary error function, and  $\{T_j\}$  are the thresholds of the receiver's scalar quantizer  $\alpha(\cdot)$  defined as

$$\begin{aligned} \alpha(z) &= j \quad \text{if } z \in (T_{j-1}, T_j), \\ T_j &= \begin{cases} -\infty & \text{if } j = -1, \\ \frac{j+1}{2^{q-2}} - 2; & \text{if } j = 0, 1, \dots, 2^q - 2, \\ +\infty & \text{if } j = 2^q - 1. \end{cases} \end{aligned} \quad (1)$$

It can be observed that the above two-input,  $2^q$ -output DMC is “weakly” symmetric in the sense that its transition probability matrix  $\mathbf{\Pi}$  can be partitioned (along its columns) into symmetric arrays – where a symmetric array is defined as an array having the property that all its rows are permutations of each others, and all its columns are permutations of each others [10, 11]. The symmetry property implies the fact that the capacity of this channel is achieved by a uniform input distribution [10]. Its capacity can therefore be easily computed by evaluating its mutual information using a uniform input distribution. In Table 1, we display the channel capacity for different values of  $q$  and the channel  $SNR$ . Note that the capacity increases with  $q$  (as expected).

### 3. COVQ DESIGN

With this simplification, we design the COVQ for the DMC using the algorithm proposed in [2]. The algorithm is an iterative algorithm which results in a locally optimal solution. We herein briefly describe it.

Consider a real-valued i.i.d. source,  $\mathcal{V} = \{V_i\}_{i=1}^\infty$ , with probability density function (p.d.f.)  $f(v)$ . The source is to be encoded by a  $k$ -dimensional,  $kr$ -bit COVQ whose output is to be transmitted over the  $2^{kr}$ -input,  $2^{qkr}$ -output DMC with transition probability distribution

$$P(\mathbf{y}|\mathbf{x}) = \prod_{l=1}^{kr} \pi_{x_l y_l},$$



Figure 2. Block Diagram of a COVQ System.

where  $\mathbf{x} \in \mathcal{X}^{kr}$  and  $\mathbf{y} \in \mathcal{Y}^{kr}$ . The encoding system, depicted in Figure 2, consists of an encoder mapping,  $\gamma$ , and a decoder mapping,  $\beta$ . The encoder mapping  $\gamma: \mathbb{R}^k \mapsto \mathcal{X}^{kr}$  is described in terms of a partition  $\mathcal{P} = \{S_{\mathbf{x}} \subset \mathbb{R}^k: \mathbf{x} \in \mathcal{X}^{kr}\}$  of  $\mathbb{R}^k$  according to

$$\gamma(\mathbf{v}) = \mathbf{x} \quad \text{if } \mathbf{v} \in S_{\mathbf{x}}, \quad \mathbf{x} \in \mathcal{X}^{kr},$$

where  $\mathbf{v} = (v_1, v_2, \dots, v_k)$  is a block of  $k$  successive source samples. The DMC takes an input sequence  $\mathbf{x}$  and produces an output sequence  $\mathbf{y}$ . It is given in terms of the block channel transition matrix  $P(\mathbf{y}|\mathbf{x})$ . Finally, the decoder mapping  $\beta: \mathcal{Y}^n \mapsto \mathbb{R}^k$  is described in terms of a codebook

$$\mathcal{C} = \{\mathbf{c}_{\mathbf{y}} \in \mathbb{R}^k: \mathbf{y} \in \mathcal{Y}^{kr}\}$$

according to

$$\beta(\mathbf{y}) = \mathbf{c}_{\mathbf{y}}, \quad \mathbf{y} \in \mathcal{Y}^{kr}.$$

The encoding rate of the above system is  $r$  bits/sample and its average squared-error distortion per sample is given by [2]:

$$D = \frac{1}{k} \sum_{\mathbf{x}} \int_{S_{\mathbf{x}}} f(\mathbf{v}) \left\{ \sum_{\mathbf{y}} P(\mathbf{y}|\mathbf{x}) \|\mathbf{v} - \mathbf{c}_{\mathbf{y}}\|^2 \right\} d\mathbf{v}, \quad (2)$$

where  $f(\mathbf{v}) = \prod_{i=1}^k f(v_i)$  is the  $k$ -dimensional source p.d.f. For a given source, channel,  $k$  and  $kr$ , we wish to minimize  $D$  by proper choice of  $\mathcal{P}$  and  $\mathcal{C}$ .

From (2), we see that for a fixed  $\mathcal{C}$  the optimal partition  $\mathcal{P}^* = \{S_{\mathbf{x}}^*\}$  is given by [2]:

$$\begin{aligned} S_{\mathbf{x}}^* &= \left\{ \mathbf{v} : \sum_{\mathbf{y}} P(\mathbf{y}|\mathbf{x}) \|\mathbf{v} - \mathbf{c}_{\mathbf{y}}\|^2 \right. \\ &\leq \left. \sum_{\mathbf{y}} P(\mathbf{y}|\tilde{\mathbf{x}}) \|\mathbf{v} - \mathbf{c}_{\mathbf{y}}\|^2, \forall \tilde{\mathbf{x}} \in \mathcal{X}^{kr} \right\}, \end{aligned}$$

$\mathbf{x} \in \mathcal{X}^{kr}$ . Similarly, the optimal codebook  $\mathcal{C}^* = \{\mathbf{c}_{\mathbf{y}}^*\}$  for a given partition is [2]:

$$\mathbf{c}_{\mathbf{y}}^* = \frac{\sum_{\mathbf{x}} P(\mathbf{y}|\mathbf{x}) \int_{S_{\mathbf{x}}} \mathbf{v} f(\mathbf{v}) d\mathbf{v}}{\sum_{\mathbf{x}} P(\mathbf{y}|\mathbf{x}) \int_{S_{\mathbf{x}}} f(\mathbf{v}) d\mathbf{v}}.$$

The above result can be easily generalized for sources with memory, e.g., a Gauss-Markov source.

#### 4. NUMERICAL RESULTS AND DISCUSSION

In Table 2, we present numerical results for the scheme in Figure 1 when the source is memoryless Gaussian. The results are given in terms of the source signal-to-quantization-noise ratio (SQNR). The numbers in brackets indicate the optimal performances theoretically attainable (OPTA) obtained by evaluating  $D(rC)$ , where  $D(\cdot)$  is the distortion-rate function of the source (for the squared-error distortion measure), and  $C$  is the capacity of the DMC derived from the AWGN channel. Here, the rate is  $r = 2$  bits/sample and the dimension is  $k = 2$ . We used 80,000 training vectors in the COVQ design program. Note that the results for  $q = 1$  correspond to hard-decision demodulation. In this case the DMC is derived from  $kr$  uses of a binary symmetric channel (BSC) with crossover probability  $Q(\sqrt{SNR})$ . Thus, for  $q = 1$ , the results in Table 1 are nearly identical to those reported in [2] for the BSC. Observe from Table 2 that the system performance increases as  $q$  increases. In this case, the largest improvement is 0.81 dB SQNR occurring at 2 dB channel SNR. Also, it can be remarked that at low channel SNR, the  $q = 4$  bit soft-decision scheme is approximately 1.3 dB in channel SNR better than the hard-decision scheme ( $q = 1$ ). For memoryless sources possessing higher amounts of redundancy, higher coding gains are achievable; for e.g., for a memoryless generalized Gaussian sources with parameter 0.5, a coding gain of 2 dB in channel SNR is obtained for  $r = 4$  and  $k = 1$ .

The cost of doing soft-decision demodulation is increased complexity. The main complexity is due to the amount of memory needed to store the look-up table in the COVQ decoder. This table includes  $2^{qkr}$  vectors — each with dimension  $k$ . The size of the table increases exponentially with  $q$ . It is hence interesting to study the behavior of the proposed system when the size of this table is constrained. In Table 3, we provide numerical results for the COVQ system when  $r = 2$  and  $qk = 4$ . In this case, the table in the COVQ decoder will always consist of 256 vectors (though the dimension of each vector is  $k$  which varies). It can be seen that at high channel SNR, the hard-decision scheme outperforms the soft-decision schemes. However at low SNR, the soft-decision schemes are superior. Furthermore, the soft-decision scheme has lower computational and storage complexity in the encoder. Also, the dimension of the vectors in the decoder table is smaller. The conclusion reached here is in general not valid for other sources. For example, we have found that for the memoryless generalized Gaussian source with parameter 0.5 and the Gauss-Markov source with correlation 0.9, the performances for  $k = 4, q = 1$  are always superior to  $k = 1, q = 4$ . This is because, for these highly-redundant sources, the high-dimension coding gain outweighs the soft-decision capacity gain.

In Tables 4 and 5, numerical results are provided for the case where the source is Gauss-Markov with correlation parameter 0.9, and with COVQ parameters  $r = k = 2$  and  $r = 2, k = 4$ , respectively. In this case, the source

has high redundancy in the form of memory. In Table 4, the results are obtained for  $q$  ranging from 1 to 4; while in Table 4, they are obtained for  $q = 1$  and 2 only. The largest improvement as  $q$  varies from 1 to 4 in Table 4 is 1.23 dB SQNR occurring at 4 dB of channel SNR. In Table 5, as  $q$  increases from 1 to 2, the largest improvement is 1.06 dB SQNR occurring at 1 dB channel SNR. The best coding gains at low channel SNR's are around 1.6 dB (Table 4) and 1.2 dB (Table 5) in channel SNR.

In Table 5, we also compare the performance of the proposed soft-decision COVQ scheme with the soft Hadamard column decoder (SHCD)<sup>3</sup> of [9]. The SHCD results in this table are for a *fixed* encoder whereas the results of the proposed scheme are for the case where *both* the encoder and decoder are *optimized* for the given channel SNR. Hence we find that even the hard-decision ( $q = 1$ ) COVQ outperforms the SHCD of [9] with a fixed encoder (optimized for the clean channel). Thus the comparison in Table 5 is not fair to [9]. In Figure 3, we attempt to make a fair comparison. In this figure, we compare the proposed soft-decision COVQ scheme with the channel-optimized SHCD scheme (both encoder and decoder are optimized for the given channel SNR) for the Gauss-Markov source with  $k = 4, r = 1$ . In this case, we find that the proposed scheme with  $q = 4$  is comparable to the channel-optimized SHCD. We observe that the decoder of the proposed scheme is just a simple table lookup while the decoder of the SHCD requires a weighted multiplication of  $2^{kr}$   $k$ -dimensional vectors. Thus, the decoder computational complexity of the proposed scheme is substantially less than SHCD. However, the decoder memory storage of the proposed scheme is  $2^q$  times more than the SHCD.

#### 5. RAYLEIGH FADING CHANNEL

In this section, we consider the channel model described by

$$z_i = a_i w_i + n_i,$$

where  $\{a_i\}$  is assumed to be i.i.d. with p.d.f.

$$f(a) = \begin{cases} 2ae^{-a^2}, & \text{if } a > 0; \\ 0, & \text{otherwise.} \end{cases}$$

Note that  $E[a_i^2] = 1$ . This channel model is often referred to as the Rayleigh fading channel model and  $a_i$  is called the channel state information (CSI). In many situations, it is assumed that  $a_i$  is known at the decoder. If the received signal  $z_i$  is normalized by  $a_i$ , we obtain

$$\tilde{z}_i = z_i/a_i = w_i + \tilde{n}_i, \quad (3)$$

where  $\tilde{n}_i = n_i/a_i$ . If  $n_i$  is zero-mean Gaussian with variance  $N_0/2$ , it can be shown that the p.d.f. of the new noise  $\tilde{n}_i$  is given by

$$f(\tilde{n}_i) = \frac{N_0/2}{(N_0 + \tilde{n}_i^2)^{3/2}}. \quad (4)$$

<sup>3</sup>The SQNR results of SHCD reported in Table 5 are approximations derived from a figure in [9].

We design a COVQ scheme for the channel modeled by (3) and (4). A two-input,  $2^q$ -output DMC is obtained from this channel using BPSK modulation and  $q$ -bit soft decision demodulation with thresholds given by (1). In Table 6, we provide the Shannon capacity (in bits/channel use) of the DMC obtained from the Rayleigh fading channel model of (3) and (4). The capacity is given as a function of the channel SNR and  $q$ . Note that the channel SNR is the received SNR as we have assumed  $E[a_i^2] = 1$ . Also observe that, beside the normalization in (4), the CSI  $a_i$  is not at all used by the decoder.

Observe that for a fixed channel SNR and a fixed  $q$ , the capacity of the DMC derived from the Rayleigh fading channel is less than the capacity of the DMC derived from the AWGN channel. Furthermore, soft-decision demodulation increases capacity relatively more in the DMC-AWGN channel case than in the DMC-Rayleigh fading channel case. As an example, at  $SNR = -1$  dB, soft-decision demodulation increases the capacity of the DMC-AWGN channel by 34% (from  $q = 1$  to  $q = 4$ ). At the same SNR, the capacity of the DMC-Rayleigh fading channel is increased by only 14%.

In Table 7, we provide numerical results for a COVQ designed for the DMC derived from the Rayleigh fading channel. These results are obtained for the memoryless Gaussian source with  $k = 2$  and  $r = 2$ . Again, we observe that the performance increases as  $q$  increases. However the soft-decision gains are not as significant as those in Table 2 due to the fact that the capacity gains in Table 6 are less than those in Table 1.

## 6. CONCLUSION

We examined the performance of a COVQ scheme over a DMC derived from soft-decision BPSK-modulated AWGN and Rayleigh fading channels. We remarked that soft-decision demodulation always yields superior performance over hard-decision demodulation. This gain comes at a cost of increased decoder memory requirement. However, we found that for the i.i.d. Gaussian source and low channel SNR's, a low-dimensional soft-decision COVQ outperforms a high-dimensional hard-decision COVQ with the same number of codevectors at the decoder. Finally, the performance of the soft-decision COVQ scheme was shown to be comparable to the soft Hadamard column decoder of Skoglund and Hedelin.

## REFERENCES

[1] H. Kumazawa, M. Kasahara, and T. Namekawa, "A Construction of Vector Quantizers for Noisy Channels," *Electronics and Engineering in Japan*, Vol. 67-B, pp. 39–47, January 1984.

[2] N. Farvardin and V. Vaishampayan, "On the Performance and Complexity of Channel-Optimized Vector Quantizers," *IEEE Transactions on Information Theory*, Vol. 37, pp. 155–160, January 1991.

[3] N. Farvardin, "A Study of Vector Quantization for Noisy Channels," *IEEE Transactions on Information Theory*, Vol. 36, pp. 799–809, July 1990.

[4] F. Alajaji, N. Phamdo, N. Farvardin and T. Fuja, "Detection of Binary Markov Sources Over Channels with Additive Markov Noise," *IEEE Transactions on Information Theory*, Vol. 42, No. 1, pp. 230–239, January 1996.

[5] F. Alajaji, N. Phamdo and T. Fuja, "Channel Codes That Exploit the Residual Redundancy in CELP-Encoded Speech", *IEEE Transactions on Speech & Audio Processing*, to appear.

[6] N. Phamdo, F. Alajaji and N. Farvardin, "Quantization of Memoryless and Gauss-Markov Sources Over Binary Markov Channels," submitted to *IEEE Transactions on Communications*, November 1994.

[7] E. Ayanoglu and R. M. Gray, "The Design of Joint Source and Channel Trellis Waveform Coders," *IEEE Transactions on Information Theory*, Vol. 33, pp. 855–865, November 1987.

[8] N. Phamdo, N. Farvardin, and T. Moriya, "A Unified Approach to Tree-Structured and Multi-Stage Vector Quantization for Noisy Channels," *IEEE Transactions on Information Theory*, Vol. 39, pp. 835–850, May 1993.

[9] M. Skoglund and P. Hedelin, "Hadamard-Based Soft-Decoding for Vector Quantization over Noisy Channels," submitted to *IEEE Transactions on Information Theory*, January 1996.

[10] R. G. Gallager, *Information Theory and Reliable Communication*, John Wiley & Sons Inc., New York, 1968.

[11] R. E. Blahut, *Principles and Practice of Information Theory*, Addison Wesley, Massachusetts, 1988.

Channel SNR	$q = 1$	$q = 2$	$q = 3$	$q = 4$
$\infty$	1.000	1.000	1.000	1.000
8.0	0.947	0.953	0.966	0.973
6.0	0.842	0.865	0.896	0.908
4.0	0.687	0.740	0.779	0.790
3.0	0.602	0.670	0.707	0.717
2.0	0.518	0.598	0.631	0.639
1.0	0.440	0.526	0.553	0.560
0.0	0.369	0.454	0.477	0.483
-1.0	0.306	0.385	0.406	0.411
-2.0	0.252	0.321	0.340	0.345
-3.0	0.206	0.264	0.280	0.285

Table 1. Capacity (in bits/channel use) of two-input,  $2^q$ -output DMC derived from BPSK-Modulated AWGN channel with  $q$ -bit soft-decision demodulation.

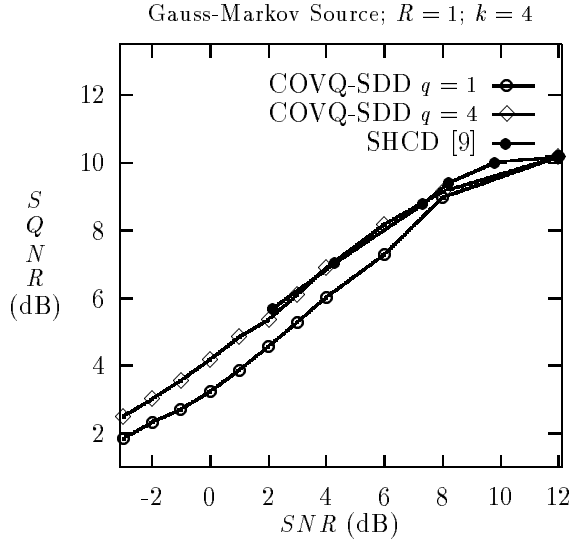


Figure 3. Performances of COVQ System in AWGN Channel with  $q = 1$  and  $q = 4$  Compared with SHCD of [9].

Channel SNR	$k = 4, q = 1$	$k = 2, q = 2$	$k = 1, q = 4$
$\infty$	10.19 [12.04]	9.55 [12.04]	9.31 [12.04]
8	8.90 [11.40]	8.59 [11.47]	8.52 [11.71]
6	7.31 [10.14]	6.88 [10.41]	7.01 [10.93]
4	5.50 [8.27]	5.51 [8.91]	5.16 [9.51]
3	4.67 [7.25]	4.86 [8.07]	4.31 [8.63]
2	3.93 [6.24]	4.21 [7.20]	3.56 [7.69]
1	3.28 [5.28]	3.64 [6.33]	3.24 [6.74]
0	2.73 [4.44]	3.11 [5.47]	3.17 [5.82]
-1	2.26 [3.68]	2.64 [4.64]	2.71 [4.95]
-2	1.86 [3.03]	2.25 [3.86]	2.28 [4.15]
-3	1.52 [2.48]	1.86 [3.18]	1.91 [3.43]

Table 3. Source SQNR (in dB) Performances of COVQ System in AWGN channel for Different Values of  $q$  (Number of Soft-Decision Bits); Memoryless Gaussian Source;  $r = 2$  Bits/Sample; Size of COVQ Decoder Table is fixed at 256. The numbers in brackets indicate the optimal performance theoretically attainable (OPTA) for the Memoryless Gaussian Source and DMC.

Channel SNR	$q = 1$	$q = 2$	$q = 3$	$q = 4$
$\infty$	9.57 [12.04]	9.57 [12.04]	9.57 [12.04]	9.57 [12.04]
8	8.64 [11.40]	8.65 [11.47]	8.69 [11.63]	8.78 [11.71]
6	6.89 [10.14]	6.94 [10.41]	7.12 [10.79]	7.28 [10.93]
4	5.17 [8.27]	5.43 [8.91]	5.78 [9.38]	5.89 [9.51]
3	4.38 [7.25]	4.87 [8.07]	5.14 [8.51]	5.23 [8.63]
2	3.77 [6.24]	4.23 [7.20]	4.46 [7.60]	4.53 [7.69]
1	3.17 [5.28]	3.65 [6.33]	3.83 [6.66]	3.88 [6.74]
0	2.66 [4.44]	3.12 [5.47]	3.27 [5.74]	3.30 [5.82]
-1	2.21 [3.68]	2.65 [4.64]	2.81 [4.89]	2.85 [4.95]
-2	1.82 [3.03]	2.26 [3.86]	2.37 [4.09]	2.40 [4.15]
-3	1.50 [2.48]	1.88 [3.18]	1.97 [3.37]	2.00 [3.43]

Table 2. Source SQNR (in dB) Performances of COVQ System in AWGN Channel for Different Values of  $q$  (Number of Soft-Decision Bits); Memoryless Gaussian Source;  $r = 2$  Bits/Sample; Dimension  $k = 2$ . The numbers in brackets indicate the optimal performance theoretically attainable (OPTA) for the Memoryless Gaussian Source and DMC (Derived from the AWGN channel).

Chan. SNR	$q = 1$	$q = 2$	$q = 3$	$q = 4$
$\infty$	13.52 [19.25]	13.52 [19.25]	13.52 [19.25]	13.52 [19.25]
8	11.11 [18.62]	11.12 [18.69]	11.22 [18.85]	11.43 [19.20]
6	8.92 [17.35]	9.21 [17.63]	9.71 [18.00]	9.94 [18.93]
4	6.96 [15.48]	7.46 [16.12]	8.02 [16.59]	8.19 [16.73]
3	6.01 [14.46]	6.56 [15.28]	7.06 [15.73]	7.20 [15.85]
2	5.14 [13.45]	5.69 [14.42]	6.08 [14.81]	6.19 [14.91]
1	4.34 [12.51]	5.18 [13.54]	5.19 [13.87]	5.25 [13.96]
0	3.62 [11.62]	4.45 [12.68]	4.70 [12.96]	4.76 [13.03]
-1	3.00 [10.76]	3.76 [11.83]	3.97 [12.09]	4.02 [12.15]
-2	2.47 [9.93]	3.13 [10.98]	3.31 [11.23]	3.35 [11.30]
-3	2.02 [9.11]	2.58 [10.13]	2.73 [10.38]	2.77 [10.45]

Table 4. Source SQNR (in dB) Performances of COVQ System in AWGN Channel for Different Values of  $q$  (Number of Soft-Decision Bits); Gauss-Markov Source with Correlation Coefficient 0.9;  $r = 2$  Bits/Sample; Dimension  $k = 2$ . The numbers in brackets indicate the optimal performance theoretically attainable (OPTA) for the Gauss-Markov Source ( $\rho = 0.9$ ) and DMC.

Chan. SNR	$q = 1$	$q = 2$	SHCD [9]
$\infty$	15.77 [19.25]	15.77 [19.25]	15.8
8	13.04 [18.62]	13.13 [18.69]	12.5
6	10.96 [17.35]	11.36 [17.63]	8.5
4	8.80 [15.48]	9.57 [16.12]	5.8
3	7.86 [14.46]	8.69 [15.28]	4.5
2	6.90 [13.45]	7.83 [14.42]	3.5
1	5.98 [12.51]	7.04 [13.54]	2.9
0	5.14 [11.62]	6.14 [12.68]	2.4
-1	4.44 [10.76]	5.32 [11.83]	1.9
-2	3.77 [9.93]	4.61 [10.98]	1.5
-3	3.17 [9.11]	3.93 [10.13]	—

Table 5. Source SQNR (in dB) Performances of COVQ System in AWGN Channel for Different Values of  $q$  (Number of Soft-Decision Bits); Gauss-Markov Source with Correlation Coefficient 0.9;  $r = 2$  Bits/Sample; Dimension  $k = 4$ . The Numbers in Brackets Indicate the Optimal Performance Theoretically Attainable (OPTA) for the Gauss-Markov Source ( $\rho = 0.9$ ) and DMC; SHCD Results are Approximations Obtained from the Figure in [9].

Channel SNR	$q = 1$	$q = 2$	$q = 3$	$q = 4$
$\infty$	1.000	1.000	1.000	1.000
16.0	0.906	0.908	0.930	0.935
14.0	0.865	0.869	0.896	0.902
12.0	0.811	0.817	0.848	0.855
10.0	0.742	0.749	0.783	0.792
8.0	0.656	0.666	0.701	0.710
6.0	0.557	0.571	0.602	0.611
4.0	0.451	0.468	0.494	0.502
3.0	0.399	0.417	0.439	0.446
2.0	0.348	0.367	0.385	0.391
1.0	0.300	0.320	0.334	0.339
0.0	0.256	0.276	0.286	0.290
-1.0	0.216	0.235	0.243	0.246
-2.0	0.181	0.198	0.204	0.206
-3.0	0.150	0.166	0.170	0.171

Table 6. Capacity (in bits/channel use) of 2-input,  $2^q$ -output DMC Derived from BPSK-Modulated Rayleigh Fading Channel with  $q$ -bit Soft-Decision Demodulation.

Channel SNR	$q = 1$	$q = 2$	$q = 3$	$q = 4$
$\infty$	9.57 [12.04]	9.57 [12.04]	9.57 [12.04]	9.57 [12.04]
16.0	7.88 [10.90]	7.89 [10.93]	8.02 [11.20]	8.08 [11.25]
14.0	7.24 [10.42]	7.25 [10.46]	7.41 [10.79]	7.48 [10.86]
12.0	6.48 [9.77]	6.49 [9.83]	6.73 [10.21]	6.81 [10.30]
10.0	5.75 [8.93]	5.79 [9.02]	6.04 [9.43]	6.13 [9.54]
8.0	4.87 [7.90]	4.93 [8.02]	5.18 [8.44]	5.26 [8.55]
6.0	4.08 [6.70]	4.16 [6.87]	4.37 [7.25]	4.44 [7.36]
4.0	3.26 [5.43]	3.36 [5.64]	3.50 [5.94]	3.56 [6.04]
3.0	2.87 [4.80]	2.98 [5.02]	3.09 [5.28]	3.14 [5.37]
2.0	2.50 [4.19]	2.62 [4.42]	2.74 [4.64]	2.78 [4.71]
1.0	2.16 [3.61]	2.29 [3.85]	2.38 [4.02]	2.42 [4.08]
0.0	1.85 [3.08]	1.98 [3.32]	2.05 [3.45]	2.07 [3.49]
-1.0	1.57 [2.60]	1.69 [2.83]	1.75 [2.92]	1.77 [2.96]
-2.0	1.32 [2.18]	1.43 [2.39]	1.48 [2.46]	1.49 [2.48]
-3.0	1.11 [1.80]	1.21 [2.00]	1.24 [2.05]	1.25 [2.06]

Table 7. Source SQNR (in dB) Performances of COVQ System in Rayleigh Fading Channel for Different Values of  $q$  (Number of Soft-Decision Bits); Memoryless Gaussian Source;  $r = 2$  Bits/Sample; Dimension  $k = 2$ . The numbers in brackets indicate the optimal performance theoretically attainable (OPTA) for the Memoryless Gaussian Source and DMC (Derived from the Rayleigh Fading Channel).